Published in final edited form as:
Mol Plant Pathol. 2013 June ; 14(5): 470–482. doi:10.1111/mpp.12020.

The actin-regulating kinase homolog MoArk1 plays pleiotropic function in *Magnaporthe oryzae*

Jiamei Wang[1], **Yan Du**[1], **Haifeng Zhang**[1], **Chen Zhou**[1], **Zhongqiang Qi**[1], **Xiaobo Zheng**[1], **Ping Wang**[2], and **Zhengguang Zhang**[1,*]

[1]Department of Plant Pathology, College of Plant Protection, Nanjing Agricultural University, and Key Laboratory of Integrated Management of Crop Diseases and Pests, Ministry of Education, Nanjing 210095, China

[2]Department of Pediatrics and the Research Institute for Children, Louisiana State University Health Sciences Center, New Orleans, Louisiana 70118, USA

Abstract

Endocytosis is an essential cellular process in eukaryotic cells that involves concord functions of clathrin and adaptor proteins, various protein and lipid kinases, phosphatases, and the actin cytoskeleton. In *Saccharomyces cerevisiae*, Ark1p is a member of the serine/threonine protein kinase (SPK) family that affects profoundly the organization of the cortical actin cytoskeleton. To study the function of MoArk1, an Ark1p homolog identified in *Magnaporthe oryzae*, we disrupted the *MoARK1* gene and characterized the Δ*Moark1* mutant strain. The Δ*Moark1* mutant exhibited various defects ranging from mycelial growth and conidial formation to appressorium-mediated host infection. The Δ*Moark1* mutant also exhibited decreased appressorium turgor pressure and attenuated virulence on rice and barley. In addition, the Δ*Moark1* mutant displayed defects in endocytosis and formation of the Spitzenkörper and was hyposensitive to exogenous oxidative stress. Moreover, a MoArk1-GFP fusion protein showed an actin-like localization pattern by localizing to the apical regions of hyphae. This pattern of localization appeared to be regulated by SNARE proteins MoSec22 and MoVam7. Finally, detailed analysis revealed that the proline-rich region within the MoArk1 S/T domain of MoArk1 was critical for endocytosis, subcellular localization and pathogenicity. These results collectively suggested that MoArk1 exhibits conserved functions in endocytosis and actin cytoskeleton organization, which may underlie growth, cell wall integrity, and virulence of the fungus.

Introduction

Eukaryotic cells internalize macromolecules and other materials from the extracellular medium through the conserved process of endocytosis. Consequentially, endocytosis serves multiple functions, including recycling of membrane proteins and lipids, internalization of membrane proteins and lipids for degradation, and internalization of signaling molecules (D'Hondt *et al*., 2000; Emans *et al*., 2002). In the budding yeast *Saccharomyces cerevisiae*, the availability of the fluorescent dye FM4-64 and Ste2p and Ste3p pheromone receptors allowed for the identification of the endocytic pathway (Toret & Drubin, 2006). Many features of the yeast endocytic pathway are also surprisingly conserved in mammalian systems (Davis *et al*., 1993; Raths *et al*., 1993). In yeasts and other fungi, either pathogenic or saprophytic, endocytosis and intracellular transport events are important for cellular functions including polarity establishment, hyphal growth, and/or virulence (Atkinson *et al*.,

*Corresponding author: Zhengguang Zhang, Dept. of Plant Pathology, College of Plant Protection, Nanjing Agricultural University, Nanjing, Jiangsu, 210095, China Tel: 86-25-84396972; Fax: 86-25-84395325; zhgzhang@njau.edu.cn.

2002; Read & Kalkman, 2003; Song *et al.*, 2010; Dou *et al.*, 2011; Shaw *et al.*, 2011; Wang & Shen, 2011). Numerous studies have examined the important roles of specific endocytic components such as *Aspergillus oryzae* End4/Sla2, *Fusarium graminearum* End1, *Ustilago maydis* Yup1 and mammalian GAK and AAK1 (Fuchs *et al.*, 2006; Higuchi *et al.*, 2009; Kim *et al.*, 2009; Smythe & Ayscough, 2003). In mammalian cells, members of the Ark/Prk family of kinases including cyclin-G-associated kinase (GAK) and adaptor-associated kinase 1 (AAK1) are important for endocytosis (Smythe & Ayscough, 2003). The roles of endocytic transport in growth and pathogenicity of *U. maydis* were also the subjects for some in depth discussions (Fuchs & Steinberg, 2005; Steinberg, 2007). The importance of endocytosis as a physiological pathway and the molecular mechanism of endocytosis have also been reported. For example, *A. nidulans* actin and myosin are important factors in endocytosis and the polarized cell growth. (Kaksonen *et al.*, 2006). In addition, phosphorylation of *A. nidulans* MyoA regulates events in the endocytic pathway, such as membrane internalization (Idrissi *et al.*, 2008; Hervas-Aguilar & Penalva, 2010). These reports further highlighted that the endocytic pathway is important for engaging in normal physiological functions in filamentous fungi, similar to other well-defined eukaryotic cells.

In rice blast fungus *Magnaporthe oryzae*, infection occurs by conidia that are composed of normally three cells. Germination of conidia involves the production of a germ tube from one or more of these cells (Howard & Valent, 1996). Endocytosis is thought to be important for conidial cells to detect certain external signals and it plays a crucial role in various aspects of hyphal tip growth (Fischer-Parton *et al.*, 2000). Successful detection for incorporation of FM4-64 into the Spitzenkörper body marked that this organelle is involved in endocytic membrane trafficking (Fischer-Parton *et al.*, 2000; Harris *et al.*, 2005; Verdin *et al.*, 2009). Despite these findings, the physiological importance and molecular process of endocytic process in filamentous fungi remains largely unaddressed and also little is known regarding the exocytotic transport of enzymes and other cell-wall lytic materials in host tissue invading processes (Gow *et al.*, 2002). We have previously characterized MoSec22 and MoVam7 as two members of the secretory soluble *N*-ethylmaleimide-sensitive factor attachment protein receptor (SNARE) complex in *M. oryz*ae, and found that they play important roles in membrane trafficking as well as in cellular growth, stress tolerance, and pathogenicity (Song *et al.*, 2010; Dou *et al.*, 2011). SNARE proteins are a family of conserved proteins involved in the intracellular transport of membrane-coated cargo from one subcellular compartment to another (Pelham, 1999). As a part of our continuing research efforts to examine the roles of membrane trafficking in fungal pathogenesis, we analyzed the physiological significance of MoArk1, the *S. cerevisiae* actin-regulating kinase 1 (Ark1) homolog in *M. oryzae*. In the present study, we demonstrated that MoArk1 regulates endocytosis and is required for conidial development, stress resistance, membrane trafficking, and pathogenicity.

Results

Identification and characterization of MoARK1

Examination of the *M. oryzae* genome database at the Broad Institute (www.broad.mit.edu/annotation/genome/magnaporthe_grisea/Home.html) revealed that MGG_11326.6 shares high amino acid sequence homology to *S. cerevisiae* Ark1p (ScArk1p) and we thus named it MoArk1. MoArk1consists of 1021 amino acid and appears to be encoded by a single copy gene. Similar to ScArk1p, MoArk1 contains a putative ser/thr kinase (S/TKc) domain in its N-terminus and three phosphorylation sites and a conserved proline-rich motif RPTAPPKP in its C-terminus (Figure S1A). MoArk1 shares 56% amino acid sequence identity with ScArk1p and 58% with *N. crassa* Ark1 homolog. In contrast, MoArk1 is less similar to human Gak1 (17%) and *Drosophila melanogaster* auxilin (15%) (Figure S1B). To address the function of MoArk1 in *M. oryzae*, the targeted gene deletion vector pMD-*MoARK1*KO

was introduced into the wild-type strain (Figure S2A) and two Δ*Moark1* mutants were confirmed by RT-PCR and Southern blot analysis (Figure S2B and S2C).

MoARK1 affects endocytosis and formation of the Spitzenkörper body

Because ScArk1p is involved in endocytosis and the actin cytoskeleton, we first evaluated whether the loss of *MoARK1* also resulted in defects in endocytosis and intracellular transport. We performed FM4-64 staining to examine vacuolar membrane internalization. In wild-type cells, visible internal staining suggested rapid uptake of the FM4-64 dye and functional endocytosis. In these cells, FM4-64 was internalized within 15 min of incubation, resulting in various bright ring-like stain structures representing endosomes and vesicles. In contrast, no definitive staining pattern was observed in the hyphae cell of the Δ*Moark1* mutant, either at the plasma membrane (PM) or in the cytosol up to 30 –45 min after exposure to the dye. Reintroduction of the *MoARK1* gene to the Δ*Moark1* mutant restored the staining pattern (Figure 1A). These results indicated that the Δ*Moark1* mutant is altered in endocytosis.

The Spitzenkörper body is a dynamic structure present at the tips of hyphal cells with a single highly polarized growth site. It is closely connected with cellular morphogenesis and polar growth and is only present at actively growing sites (Virag & Harris, 2006). Recent studies suggested that the Spitzenkörper is involved in both exocytosis and endocytosis. To examine whether the endocytosis defect of the Δ*Moark1* mutation also affects Spitzenkörper formation, we observed Spitzenkörper formation using FM4-64 staining. The Spitzenkörper was readily visible within 15 min of incubation in the wild-type strain, but not in the Δ*Moark1* mutants even after the extended incubation time (Figure 1B), suggesting that disruption of *MoARK1* resulted in defects in Spitzenkörper formation.

Growth defects of ΔMoark1 mutants on various media

Given that ScArk1p was identified relevant to the growth characteristics of the yeast cell (Smythe & Ayscough, 2003), we investigated whether MoArk1 has a similar role. After incubation at 28°C for 7 days in the dark, the Δ*Moark1* mutant showed reduced growth rates, sparse aerial mycelia, and abnormal pigmentation on various media including CM, OM, SDC, and V8 (Figure 2A). This suggests that loss of MoArk1 maybe reduce fitness of the Δ*Moark1* mutant. Dry weight of the mycelium, which was incubated in CM media for 48 h was significantly reduced by > 30% when comparing to the wild type, indicating that MoArk1 is important for growth (Figure 2B). To determine whether deletion of MoArk1 affected growth on complex media, wild type Guy11, ΔΔ*Moark1* mutant and the complemented strains were cultured on GMM or FMM media containing different carbon and nitrogen sources, such as vitamins (VA), casamino acids (CA), peptone (PE), yeast extract (YE), yeast nitrogen base without amino acids (YN-AA), $NaNO_3$ or $(NH_4)_2SO_4$. The results showed that the Δ*Moark1* mutant grow much slower than that of wild type and the complemented strains (on GMM+VA, GMM+CA, GMM+PE, GMM+ $NaNO_3$ and FMM+ $NaNO_3$ media, Figure 2C and 2D). In contrast, no significant difference was observed between wild type and the Δ*Moark1* mutant on GMM+YE, GMM+YE-AA and FMM+ $(NH_4)_2SO_4$ media (Figure 2C and 2D). These results indicated that MoArk1 play a crucial role in nutrient uptake.

MoArk1 disruption resulted in reduction in conidia formation and abnormal conidium morphology

Conidia play an important role in the disease cycle of rice blast (Lee *et al.*, 2006). To examine the role of MoArk1 in conidium production, conidiation of the wild-type strain (Guy11), Δ*Moark1* mutants (#2 and #4), and the complemented strain (Δ*Moark1/MoARK1*) from 7-day-old SDC culture were examined. Conidia formation was reduced by

approximately two- to three folds in the Δ*Moark1* mutants compared with the wild type and complemented strains (Figure 3A, 3B and 3C). Some of the conidia formed by Δ*Moark1* mutants also had abnormal morphology. CFW staining showed that 30% of the mutant conidia had only one or two cells, in contrast to the mostly (~95%) three celled conidia of the wild type (Figure 3D). Surprisingly, we found that Δ*Moark1* mutants showed no obvious defect in conidium germination and appressorium formation. These results suggested that loss of MoArk1 affects conidiogenesis and conidial morphology.

MoArk1 directly or indirectly contributes to pathogenicity of M. oryzae

To determine whether MoArk1 is involved in pathogenesis, conidial suspensions (5×10^4 spores/ml) from the wild type, two independently generated Δ*Moark1* mutants, and complemented strains were sprayed onto susceptible rice seedlings (CO-39 cv. *oryzae*) and detached barley leaves. After 7 days, the Δ*Moark1* mutants could still cause disease lesions, but a significant reduction in lesion numbers was found compared to those produced by the controls (Figure 4A). Disease on rice was also quantified using a “lesion-type” scoring assay (Valent *et al.*, 1991) that showed, while lesion types 1–3 were produced by both the Δ*Moark1* mutants and wild type, lesion types 4 and 5 (severe, coalescing) were not produced by the mutant (Figure 4B). On detached barley leaves, which were inoculated with three different concentrations of conidial suspensions (1×10^5, 1×10^4, 1×10^3 spores/ml), lesions produced by the Δ*Moark1* mutants were less severe (Figure 4C). Thus, loss of MoArk1 function reduces colonization of leaves by the rice blast fungus.

ΔMoark1 mutants were altered in generating appressorium turgor pressure

To penetrate the rice leaf cuticle and cause infection, a high appressorium internal turgor pressure is required (Thines *et al.*, 2000; Talbot and Foster, 2001). Appressorium turgor can be measured using an incipient cytorrhysis assay, which uses hyperosmotic concentrations of a solute to collapse the appressoria (DeJong *et al.*, 1997). Since appressorial formation appears to be normal in the Δ*Moark1* mutants (Figure 4D), we hypothesized that the reduced pathogenicity may be due to a defect in appressorium turgor pressure. The appressoria of the Δ*Moark1* mutants showed an increased collapse rate even in 1 M glycerol solution (Figure 4E), validating our hypothesis. We further inoculated the conidial suspensions onto onion epidermises and found that only a small number of appressoria were developed after 48 h (approximately 30% comparing with 95% in the wild type) (Figure 4F). The wild type strain exhibited an approximately 85% penetration rate, while the penetration rate of the Δ*Moark1* mutants was only 30%. The percentage of infectious hyphae in the wild type was also distinct from the Δ*Moark1* mutant (Figure 4G). These results indicated that the reduced pathogenicity of the Δ*Moark1* mutant was due at least in part to defects in appressorium turgor pressure and subsequent host penetration.

ΔMoark1 mutants were defective in infectious hyphae growth on plant

To further explore the reasons that Δ*Moark1* mutants reduced virulence on host plants, we examined the invasive hyphae growth on both barley leaves and rice leaf sheath. After incubation with the spore suspensions for 48 h, four types (Type1: no penetration, type 2: with penetration peg, type 3: with a single invasive hyphae, type 4: with extensive hyphae growth) of invasive hyphae were observed in barley tissues (Figure 5A). In the wild type Guy11 and the complemented strains, 60% cells showed type 4 and 18% showed type 1 and type2 invasive hyphae growth. In contrast, less than 10% cell showed type 4 and more than 80% showed type 1 and type2 invasive hyphae growth in the Δ*Moark1* mutants. Additionally, the proline rich domain deletion mutant 40% cells showed type4 and 20% showed type1 and type2 (Figure 5A and 5B). The similar result was observed in the rice leaf sheath, the wild type Guy11 and complemented strains displayed faster hyphae growth extension to neighboring cells, while the Δ*Moark1* mutants showed lower hyphae growth

limited in one cell (Figure 5C). These results indicated that MoArk1 have an important role in infectious hyphae growth and plant conolization.

ΔMoark1 mutants are less sensitive to salt and osmotic stress

To investigate the role of MoArk1 in stress responses such as sensitivity to salt and osmotic adaptation, the wild-type Guy11, Δ*Moark1*, and complemented strains were exposed to various conditions including ion stress (Na^+ and K^+) and osmotic stress (sorbitol). The Δ*Moark1* mutant exposed to 0.7 M NaCl, 1 M sorbitol, and 1.2 M KCl, respectively, had a 20%, 8%, and 45% lower growth inhibition than the wild-type strain (Figure S3A and S3B). This demonstrates that the lack of MoArk1 affects salt and osmotic adaptation.

Cell wall integrity is altered in the ΔMoark1 mutants

As the fungal cell wall plays an essential role in maintaining hyphal morphology and adaptation to the environment, the structural integrity of the Δ*Moark1* mutant cell wall and membrane was examined. Mycelial growth was measured on CM medium containing various concentrations of cell wall stressors including CFW, SDS, and CR. In growth assays with three different concentrations of CFW, the Δ*Moark1* mutant showed slight resistance to CFW with an average 8%, 10%, and 12% lower growth inhibition than the wild type and complemented strains, which were 30%, 40% and 50%, respectively (Figure S4A and S4B). The responses to SDS and CR were slightly different. At lower concentrations, the Δ*Moark1* mutants showed sensitivity to these stress inducers, but at higher concentrations, the mutants showed more resistance (Figure S4C, S4D, and S4E). The results were largely supportive of our hypothesis that MoArk1 plays a role in cell wall integrity.

Deletion of MoARK1 alters chitin distribution

Previous studies have shown that Δ*Movam7* and Δ*Mosec22* mutants exhibited abnormal chitin distributions, which were not restricted to growing apices but also on lateral walls along hyphal axes. In the wild-type *M. oryzae* strain, CFW fluorescence was mostly distributed at the septa and tips where chitin, one of main components of the fungal cell wall, was actively synthesized. In the Δ*Moark1* mutants, patches of bright fluorescence were observed on the lateral wall of hyphae in addition to septa and hyphal tips (Figure 6A). This abnormal distribution of cell wall components was restored by reintroduction of wild-type MoArk1 (Figure 6A). Due to continuous tip elongation in filamentous fungi, these organisms may need to recycle certain components, such as cell wall-building enzymes, to the tip region. As CFW intercalates with nascent chitin chains, this result suggests that the altered distribution of chitin on the Δ*Moark1* mutant cell wall could be due to aberrant cell wall synthesis activities.

Additionally, we examined the effects of lytic enzymes (10 mg/ml lysing enzymes) on the Δ*Moark1* mutant. More protoplasts were found in the Δ*Moark1* mutant than the controls after treatment for 60 and 90 min (Figure 6B). When observed at 60 min, the Δ*Moark1* mutant showed a greater number of protoplasts and almost no mycelia fragments were observed, in contrast the wild type where mycelial fragments were still found (Figure 6C).

ΔMoark1 mutants are less sensitive to oxidative stress and exhibit higher extracellular peroxidase activities

In fungi, secreted peroxidases are regarded as an important component to help pathogens detoxify host-derived reactive oxygen species during plant–microbe interactions (Guo *et al.*, 2010). To investigate whether MoArk1 was involved in the oxidative stress response, wild-type Guy11, Δ*Moark1* mutants, and the complemented strains were exposed to hydrogen peroxide (H_2O_2). The mycelial growth of the Δ*Moark1* mutants was slightly affected

(Figure S5A). Exposure to 2.5 and 5 mM H_2O_2 led to an average 5% (2.5 mM) and 13% (5 mM) decrease, respectively, in growth inhibition compared to the wild-type strain (Figure S5B).

We next evaluated the influence of H_2O_2 on CR degradation as indicated by the presence of discolored halos surrounding the colony. Discolored halos were observed in the Δ*Moark1* mutants and the control strain (Figure S5C). The discoloration appeared to be more solid than the wild type, suggesting that MoArk1 might also affect the peroxidase activity. Indeed, enzyme activity assays using extracellular culture filtrates and ABTS as a substrate revealed that the Δ*Moark1* mutant exhibited the stronger peroxidase activity (Figure S5D). We further examined the transcriptional levels of four peroxidase-encoding genes all of which possess a signal peptide (MGG_04545.6, MGG_13291.6, MGG_08730.6, and MGG_07790.6). We found that the expression levels for three of these genes were increased in the Δ*Moark1* mutants (Figure S5D). These data suggested that MoArk1 is involved in controlling extracellular peroxidase activities by negative feedback regulation.

A proline-rich motif is responsible for the subcellular localization of MoArk1

In *S. cerevisiae*, Ark1p was found to affect the organization of the cortical actin cytoskeleton. Actin plays multiple complex roles in cell growth and cell shape (Heath *et al.*, 2003). Recently, actin patches, which represent sites of endocytosis, were demonstrated to be present in a subapical collar at the growing tips of hyphae and germ tubes of filamentous fungi. This zone of endocytosis is now known to be necessary for filamentous growth to proceed (Kaksonen *et al.*, 2003). A ScArk1p-GFP fusion protein was visible in the cortical patch structure with a very similar appearance and behavior to actin patches. When GFP and actin were both visualized by indirect immuno-fluorescence, they were found to co-localize in patches at the cell cortex (Smythe & Ayscough, 2003). To investigate whether MoArk1 exhibits the actin-like distribution pattern, we detected the subcellular localization of MoArk1 using a *MoARK1*-GFP fusion protein. In Δ*Moark1* expressing MoArk1-GFP, fluorescence was detected mainly in vacuole-like or patches in vegetative hyphae tips. Meanwhile, the hyphae were stained with rhodamine–phalloidin that binds actin after 48 h static culture, which showed red fluorescence co-localizing with MoArk1-GFP fluorescence (Figure 7A). During appressoria development, fluorescent signals were also detected on the periphery of appressoria and in vacuoles. In mature appressoria (24 h), GFP signals were mainly localized to globular structures at the base of mature appressoria (Figure 7B).

Proline-rich (KPxPPPKP) regions are known to mediate protein–protein interactions and can be bound by Src-homology (SH3) domains (Cope *et al.*, 1999). Several interactions involving proline-rich motifs and SH3 domains are found among proteins in yeast cortical actin patches. MoArk1 may also participate in such associations. We generated the *MoARK1*$^{\Delta RPTAPPKP}$-GFP construct and transformed it into Δ*Moark1* protoplasts. In the resulting transformants, the GFP fluorescence was weaker and the Ark1 localization pattern was not observed in hyphae and mature appressoria compared to the *MoARK1*-GFP transformants (Figure 7C and 7D). We also examined the GFP signal during infection, the *MoARK1*-GFP remain showed an actin-like localization pattern in the plant cells. However, only dispersed GFP signal was observed in the *MoARK1*$^{\Delta RPTAPPKP}$-GFP and *MoARK1*$^{\Delta S\_TKc}$-GFP transformants (Figure 7E). The above results indicated that the proline-rich region is responsible for the subcellular localization of MoArk1 as well as pathogenicity.

MoArk1 subcellular localization involves functions of SNARE proteins MoVam7 and MoSec22

SNARE proteins ensure specific recognition and transportation of vesicles and target membrane-mediated fusions (Fukuda *et al.*, 2000). Our previous studies identified two SNARE proteins, MoVam7 and MoSec22, which are involved in cell membrane transport and endocytosis (Song *et al.*, 2010; Dou *et al.*, 2011). To determine whether MoVam7 and MoSec22 are involved in the subcellular localization of MoArk1, we transformed *MoARK1*-GFP into the Δ*Mosec22* and Δ*Movam7* mutants. We found that GFP fluorescence was clustered at the hyphae tip in the Δ*Moark1*/*MoARK1* complemented strain. In contrast, the fluorescence was primarily internal in the hyphae of Δ*Mosec22*/*MoARK1*-GFP and Δ*Movam7*/*MoARK1*-GFP mutants (Figure 7F). This suggests that the lack of MoSec22 and MoVam7 disturb vesicle transport, which affects the proper MoArk1 localization.

Functional characterization of different domains of the MoARK1

MoARK1 has an S/TKc domain and a RPTAPPKP motif, similar to ScArk1p. We also generated mutant alleles of *MoARK1*-GFP (Figure 8A). Transformants expressing the MoArk$^{\Delta S/TKc}$-GFP had similar phenotypes to Δ*Moark1*, which showed reduction in plant infection and altered endocytosis (Figure 8B and 8C). This indicated that both S/TKc domain and RPTAPPKP motif is essential for the role of MoArk1 in endocytosis and virulence.

Discussion

Endocytosis is the process by which eukaryotic cells internalize macromolecules containing plasma membrane lipids and associated proteins in vesicles that fuse with the endosomal system. Subsequent sorting into different endosomal domains determines whether a given cargo recycles to the PM, traffics to the Golgi, or follows the endocytic pathway to the vacuolar lumen, undergoing degradation. *S. cerevisiae* played a key role in our understanding of the endocytic internalization process and ScArk1p is one of the proteins that regulate endocytosis through binding to other cortical actin cytoskeleton proteins. As a serine/threonine kinase, ScArk1p initiates phosphorylation cycles that control the endocytic machinery. Here, we characterized *MoARK1*, a ScArk1 homolog from *M. oryzae* and found that it too plays a role in the regulation of endocytosis and the actin cytoskeleton. We conferred that such important functions endow MoArk1 a role in growth, cell wall integrity, and virulence.

MoArk1 plays a role in cell wall integrity of M. oryzae

In *M. oryzae*, the cell wall undergoes considerable changes during morphogenesis (Jeon *et al.*, 2008). Previous studies have revealed that most cell wall defective mutants with breached cell wall integrity exhibited various developmental defects and were nonpathogenic (Li *et al.*, 2006; Jeon *et al.*, 2008). Also, the polarized growth of filamentous fungi has been speculated to require the endocytic uptake and recycling of cell wall components such as chitin (Harris, 2006). Multiple signaling pathways allow organisms to respond to different extracellular stimulus and to adjust their cellular machinery according to changes in their environment. Sensing changes in environmental osmolarity is vital for cell survival. Several cell wall integrity-associated genes such as MoMck1, MoPdeH and MoRgs1 have been characterized in *M. oryzae* (Jeon *et al.*, 2008; Zhang *et al.*, 2011b; Zhang *et al.*, 2011a), which have been described as being essential for cell wall integrity and pathogenicity. Consistent with these studies, we found that the weakened cell walls and membranes were coupled with abnormal distribution of chitins in the Δ*Moark1* mutants. Thus, disruption of normal membrane trafficking by MoArk1 may negatively affect the

secretory transport of chitosomes containing chitins and the enzymes that synthesize chitin. Meanwhile, the Δ*Moark1* mutant exhibited somewhat resistance to cell wall stress-inducing agents at higher concentrations such as CFW that may result from changes in cell wall metabolism/composition or compensatory function by other S/T kinases.

MoSec22 and MoVam7 are SNARE homologs in *M. oryzae* (Song *et al.*, 2010; Dou *et al.*, 2011). Targeted deletion of MoSec22 and MoVam7 resulted in numerous developmental defects, including cell wall integrity, which very similar to the ecology phenotype of the Δ*Moark1* mutants. Thus, endocytosis signaling may have cross talk with MAPK signaling in regulating cell wall integrity. In *A. oryzae*, the homolog of *S. cerevisiae* End4/Sla2 is AoEnd4. Hyphae grown under *AoEND4*-repressed conditions displayed marketed growth defect and irregular-shaped colonies as the result of apical growth defects, endocytic defects in FM4-64, and abnormal cell wall synthesis. Calcofluor white staining revealed that chitin accumulated in aberrant invagination structures under *AoEND4*-repressed conditions (Higuchi *et al.*, 2009). These results suggested that proteins involved in cell wall synthesis, such as chitin synthases, are not likely recycled to the tip region and therefore accumulate in the aberrant invagination structures. Overall, this is consistent with that endocytosis plays a crucial role in the physiology of hyphal growth and maintenance of cell wall integrity.

Effects of MoArk1 in endocytosis and pathogenicity

Studies in *S. cerevisiae* have demonstrated the importance of intracellular transport in the growth and differentiation of lower eukaryotic organisms. As secretory properties in particular have the propensity to be linked to virulence, intracellular transport in medically important pathogenic fungi, such as *Candida albicans* and *Cryptococcus neoformans*, has been the focus of several studies (Chaffin *et al.*, 1998). In *C. neoformans*, deletion of endocytic protein Cin1 resulted in mutant strains with reduced pathogenicity and pleiotropic defects including reduced melanin production (Shen et al., 2011). In *M. oryzae*, defects in cell-wall composition can influence appressorium formation and impair successful infection of rice (Skamnioti *et al.*, 2007). During hyphal growth and appressorium formation, endocytic markers were actively internalized by both conidia and conidial germlings on rice leaves, suggesting that endocytosis might play a major role in spore germination and growth of the germ tube.

FM4-64 staining revealed that endocytosis was blocked by disruption of *MoARK1*, and the Δ*Moark1* mutants also failed to display the Spitzenkörper body, the structure associated with rapidly growing hyphal tips in filamentous fungi. Meanwhile, the Δ*Moark1* mutant had infection defects on plants. During the extreme polarized growth of fungal hyphae, secretory vesicles are thought to accumulate in a subapical region called the Spitzenkörper. In Δ*Moark1* mutants, the secretory vesicles and endosome may have failed to accumulate due to the lack of the Spitzenkörper body, as well as abnormal appressorium formation, which is a terminal cell required for penetration of the host that is formed from the germ tube tip. This indicates that growth and differentiation were compromised in the Δ*Moark1* mutants, which would likely have reduced pathogenicity on host plants due to the loss of endocytosis and abnormal appressoria.

The balance between endocytosis and exocytosis in M. oryzae

The Apical Recycling Model predicts that a balance between exocytic and endocytic processes must be present at the hyphal tip to allow for growth, and when exocytosis and endocytosis are in balance, the resulting cell shape is a hypha (Shaw *et al.*, 2011). Accordingly, the conidium shape of the Δ*Moark1* mutants displayed abnormal morphology, indicating that exocytosis and endocytosis may function in overlapping but distinct pathways that regulate the intracellular trafficking in *M. oryzae*. When endocytosis was

down-regulated or abolished, as in the *slaB*, *fimA*, and *arfB* mutants in *Aspergillus*, the cell was unable to maintain polarity (Lee *et al.*, 2008; Upadhyay & Shaw, 2008; Hervas-Aguilar & Penalva, 2010). In contrast, when endocytosis is unaffected, the actin patches are present at the cell apex, hyphal growth ceases as the polarization machinery is cycled back into the cell. Since a precise balance between exocytosis and endocytosis exists at the hyphal tip, one can further predict that the fungal cell could alter this balance to undergo morphogenic changes. In *M. oryzae*, both the Δ*Movam7* and the Δ*Mosec22* mutants are defective in conidiogenesis and appressorium formation; they failed to colonize plant tissue and were not able to form conidiophores, suggesting that vesicular trafficking mediated by different SNAREs is dependent on the stage of conidiogenesis. Meanwhile, the SNARE proteins MoVam7 and MoSec22 are involved in the subcellular localization of MoArk1. Future studies on the intracellular trafficking of the endocytic pathway and the balance between endocytosis and exocytosis are warranted.

In summary, we found that MoArk1 is a multifunctional protein required for conidiogenesis and pathogenicity in *M. oryzae*. MoArk1 participates in the maintenance of cell wall integrity and intracellular trafficking. While the precise role of MoArk1 in regulating endocytosis remains the subject of future studies, the multifunction of MoArk1 underscores the importance of endocytic proteins in the physiology and pathogenicity of fungi. Further studies to dissect proteins that interact with MoArk1 and to delineate the significance of these interactions will reveal the importance of endocytosis in virulence mechanisms of *M. oryzae*.

Materials and Methods

Strains and culture conditions

M. oryzae strain Guy11 was used as the parental strain and all of the strains were cultured on complete medium (CM) at 28°C unless stated otherwise. Liquid CM medium was used to prepare the mycelia for DNA and RNA extraction. For conidiation, strain blocks were maintained on straw decoction and corn agar media (SDC: 100 g of straw, 40 g of corn powder, 15 g of agar in 1 L of distilled water) at 28°C for 7 days in the dark followed by 3 days of continuous illumination under fluorescent light. For medium containing cell wall perturbing agents, the final concentrations were 0.005-, 0.01-, and 0.02% for sodium dodecyl sulfate (SDS), 200-, 400- and 600 μg/ml for Congo Red (CR), and 200-, 400-, 600 μg/ml for Calcofluor White (CFW).

MoARK1 cloning and sequence analysis

A full-length cDNA fragment for the *MoARK1* gene was isolated from Guy11 strain. cDNA was cloned into pMD19 T-vector (TaKaRa, Dalian, China) to generate pMD-*MoARK1* and verified by sequencing. Amino acid sequence alignments were performed using the Clustal_W program and the calculated phylogenetic tree was viewed using Mega 3.1 Beta program.

Disruption of MoARK1 and the ΔMoark1 mutant complementation

The vector pMD-*MoARK1* was constructed for targeted gene deletion by inserting the hygromycin resistance *HPH* marker gene cassette into the two flanking sequences of the *MoARK1* gene (Figure S2A). A 1.0 kb upstream flanking sequence and a 1.1 kb downstream flanking sequence were amplified with primer pairs FL8678/FL8679 and FL8680/FL8681, respectively. Two PCR fragments were linked by overlap PCR with primer pairs FL8678/FL8681, and the linked sequence cloned into pMD19 T-vector. The *HPH* gene cassette, amplified with primers FL1111/FL1112, was inserted into pMD-*MoARK1* at the *Pme*I site to generate the final pMD-*MoARK1*KO. A 3.5 kb fragment containing the

MoARK1 disruption allele was amplified using primers FL8678/FL8681, purified, and used to transform Guy11 according to established protocols. Table S1 lists all of the primers used.

Putative Δ*Moark1* mutants were screened by PCR and confirmed by Southern blotting analysis (Figure S2B and S2C). Further confirmation was done through RT-PCR with primers FL8682/FL8683. For complementation, a 4.9 kb PCR product containing the full-length *MoARK1* coding region and the 1.5 kb upstream region, was amplified using primers FL9653/FL9654 and subcloned into pYF11 generating pYF11-*MoARK1R*. The resulting transformants were first screened by phenotype characterization followed by PCR amplification and verified by fully restored growth.

Assays for dry weight, protoplast release, vegetative growth, conidiation and appressorium formation

For vegetative growth, mycelia plugs of 3 mm × 3 mm were transferred from 7-day-old CM plates and inoculated on fresh media (CM, V8, OM, and SDC) (Zhang *et al.*, 2010) followed by incubation at 28°C. The radial growth was measured after incubation for 6 days. All experiments were repeated three times each with three replicates. For conidia production, mycelia were grown in the dark on SDC medium at 28°C for 7 days followed by constant illumination for 3–4 days. Conidia were collected by washing with double distilled water (ddH_2O), filtered through three-layer lens paper, and concentrated by centrifugation (6,000 g) for 10 min. The final spores were suspended into 2 ml ddH_2O and counted using a hemacytometer.

Appressorium formation was measured on Gel Bond film (FMC Bioproducts, Rockland, Maine, USA) as previously described (Zhang *et al.*, 2011c). Appressoria were observed through direct microscopic examination and percentages obtained from at least 100 conidia per replicate at 24 and 48 h in at least three experiments.

Light microscopy studies

To examine hyphal morphology, strains were grown on a thin layer of CM agar on the microscope slides. After 2 days in a 28°C growth chamber, the hyphae were observed under an Olympus BH-2 microscope (Olympus, Japan). The cell wall, hyphal septum, and conidia were visualized by CFW (10 μg/ml, Sigma) staining as described (Harris *et al.*, 1994). FM4-64 staining was conducted following procedures previously described (Fischer-Parton et al., 2000). Fluorescence microscopy was performed using a laser scan confocal microscopy.

Pathogenicity assay

Conidia were harvested from 10-day-old SDC agar cultures, then filtered through three layers of lens paper, and resuspended to a concentration of 5×10^4 spores/ml in a 0.2% (w/v) gelatin solution. For the detached-leaf assay, the leaves from 7-day-old barley (cv. Four-arris) seedlings were used. Two-week-old seedlings of rice (*Oryzae* sativa cv. CO39) and 7-day-old seedlings of barley were used for the infection assays. Three 20 μl droplets were placed onto the upper side of the barley leaves maintained on 4% (w/v) water agar (WA) plates. Pictures were taken 5 days after incubation at 25°C. For spray inoculation, 5 ml of conidial suspension of each treatment was sprayed onto rice with a sprayer. Inoculated plants were kept in a growth chamber at 25°C with 90% humidity and in the dark for the first 24 h, followed by a 12/12 h light/dark cycle. Lesion formation was observed daily and photographed 7 days after inoculation.

Measurement of the chitin content

Chitin (N-acetylglucosamine, GlcNAc) content was determined as described (Bulik *et al.*, 2003). Briefly, for each sample, 5 mg of freeze dried mycelia was resuspended in 1 ml 6% KOH and heated at 80°C for 90 min. Samples were centrifuged (16,000 g, 10 min) and pellets washed with PBS in three cycles of centrifugation and suspension (16,000 g, 10 min) before final suspension in 0.5 ml of McIlvaine's buffer (pH 6). 100 μl (13 units) of *Streptomyces plicatus* chitinase (Sigma) was added and incubation was for 16 h at 37°C with gentle mixing. 100 μl samples were then combined with 100 μl of 0.27 M sodium borate (pH 9), heated for 10 min at 100°C, and 1 ml of freshly diluted (1:10) of Ehrlich's reagent (10 g p-dimethylaminobenzaldehyde in 1.25 ml of HCl and 8.75 ml glacial acetic acid) was added. After incubating at 37°C for 20 min, 1 ml of the sample was transferred to a 2.5 ml plastic cuvette (Greiner) and the absorbance at 585 nm was recorded. Standard curves were prepared with GlcNAc (Sigma, USA). The experiment was repeated three times.

Supplementary Material

Refer to Web version on PubMed Central for supplementary material.

Acknowledgments

This research was supported by the National Basic Research Program of China (Grant No: 2012CB114000 to ZZ), Natural Science Foundation of China (Grant No: 31271998 to ZZ, 30971890 to XZ), the Fundamental Research Funds for the Central Universities (Grant No: KYZ201105 to ZZ), and the Project of Jiangsu of China (Grant No: Sx (2009) 54 to XZ). Research in Wang laboratory was supported by US grants (NIH/NIAID AI054958 and AI074001).

Reference

Anton J, Rossello-Mora R, Rodriguez-Valera F, Amann R. Extremely halophilic bacteria in crystallizer ponds from solar salterns. Appl. Environ. Microbiol. 2000; 66:3052–3057. [PubMed: 10877805]

Atkinson HA, Daniels A, Read ND. Live-cell imaging of endocytosis during conidial germination in the rice blast fungus, *Magnaporthe grisea*. Fungal Genet. Biol. 2002; 37:233–244. [PubMed: 12431458]

Bulik DA, Olczak M, Lucero HA, Osmond BC, Robbins PW, Specht CA. Chitin synthesis in *Saccharomyces cerevisiae* in response to supplementation of growth medium with glucosamine and cell wall stress. Eukaryot. Cell. 2003; 2:886–900. [PubMed: 14555471]

Chaffin WL, Lopez-Ribot JL, Casanova M, Gozalbo D, Martinez JP. Cell wall and secreted proteins of *Candida albicans*: Identification, function, and expression. Microbiol. Mol. Biology Rev. 1998; 62:130–180.

Cope MJ, Yang S, Shang C, Drubin DG. Novel protein kinases Ark1p and Prk1p associate with and regulate the cortical actin cytoskeleton in budding yeast. J. Cell Biol. 1999; 144:1203–1218. [PubMed: 10087264]

D'Hondt K, Heese-Peck A, Riezman H. Protein and lipid requirements for endocytosis. Annu. Rev. Genet. 2000; 34:255–295. [PubMed: 11092829]

Davis NG, Horecka JL, Sprague GF Jr. Cis- and trans-acting functions required for endocytosis of the yeast pheromone receptors. J. Cell Biol. 1993; 122:53–65. [PubMed: 8391002]

DeJong JC, MCCormack BJ, Smirnoff N, Talbot NJ. Glycerol generates turgor in rice blast. Nature. 1997; 389:244–245.

Dou XY, Wang Q, Qi ZQ, Song WW, Wang W, Guo M, Zhang HF, Zhang ZG, Wang P, Zheng XB. MoVam7, a conserved SNARE involved in vacuole assembly, is required for growth, endocytosis, ROS accumulation, and pathogenesis of *Magnaporthe oryzae*. PLoS One. 2011; 6:e16439. [PubMed: 21283626]

Emans N, Zimmermann S, Fischer R. Uptake of a fluorescent marker in plant cells is sensitive to brefeldin A and wortmannin. Plant Cell. 2002; 14:71–86. [PubMed: 11826300]

Fischer-Parton S, Parton RM, Hickey PC, Dijksterhuis J, Atkinson HA, Read ND. Confocal microscopy of FM4-64 as a tool for analysing endocytosis and vesicle trafficking in living fungal hyphae. J. Microsc-Oxford. 2000; 198:246–259.

Fuchs U, Hause G, Schuchardt I, Steinberg G. Endocytosis is essential for pathogenic development in the corn smut fungus *Ustilago maydis*. Plant Cell. 2006; 18:2066–2081. [PubMed: 16798890]

Fuchs U, Steinberg G. Endocytosis in the plant-pathogenic fungus *Ustilago maydis*. Protoplasma. 2005; 226:75–80. [PubMed: 16231103]

Fukuda R, McNew JA, Weber T, Parlati F, Engel T, Nickel W, Rothman JE, Sollner TH. Functional architecture of an intracellular membrane t-SNARE. Nature. 2000; 407:198–202. [PubMed: 11001059]

Galletta BJ, Cooper JA. Actin and endocytosis: mechanisms and phylogeny. Curr. Opin. Cell Biol. 2009; 21:20–27. [PubMed: 19186047]

Gow NAR, Brown AJP, Odds FC. Fungal morphogenesis and host invasion. Curr. Opin. Microbiol. 2002; 5:366–371. [PubMed: 12160854]

Guo M, Chen Y, Du Y, Dong YH, Guo W, Zhai S, Zhang HF, Dong SM, Zhang ZG, Wang YC, Wang P, Zheng XB. The bZIP Transcription factor MoAP1 mediates the oxidative stress response and is critical for pathogenicity of the rice blast fungus *Magnaporthe oryzae*. PLoS Pathog. 2011; 7:e1001302. [PubMed: 21383978]

Guo M, Guo W, Chen Y, Dong SM, Zhang XB, Zhang HF, Song WW, Wang W, Lv RL, Zhang ZG, Wang YC, Zheng XB. The basic leucine zipper transcription factor Moatf1 mediates oxidative stress responses and is necessary for full virulence of the rice blast fungus *Magnaporthe oryzae*. Mol. Plant Microbe Interact. 2010; 23:1053–1068. [PubMed: 20615116]

Harris SD. Cell polarity in filamentous fungi: shaping the mold. Int. Rev. Cytol. 2006; 251:41–77. [PubMed: 16939777]

Harris SD, Morrell JL, Hamer JE. Identification and characterization of *Aspergillus nidulans* mutants defective in cytokinesis. Genetics. 1994; 136:517–532. [PubMed: 8150280]

Harris SD, Read ND, Roberson RW, Shaw B, Seiler S, Plamann M, et al. Polarisome meets spitzenkörper: microscopy, genetics, and genomics converge. Eukaryot. Cell. 2005; 4:225–229. [PubMed: 15701784]

Heath IB, Bonham M, Akram A, Gupta GD. The interrelationships of actin and hyphal tip growth in the ascomycete *Geotrichum candidum*. Fungal Genet Biol. 2003; 38:85–97. [PubMed: 12553939]

Hervas-Aguilar A, Penalva MA. Endocytic machinery protein SlaB is dispensable for polarity establishment but necessary for polarity maintenance in hyphal tip cells of *Aspergillus nidulans*. Eukaryot. Cell. 2010; 9:1504–1518. [PubMed: 20693304]

Higuchi Y, Shoji JY, Arioka M, Kitamoto K. Endocytosis is crucial for cell polarity and apical membrane recycling in the filamentous fungus *Aspergillus oryzae*. Eukaryot. Cell. 2009; 8:37–46. [PubMed: 19028995]

Hoffmann J, Mendgen K. Endocytosis and membrane turnover in the germ tube of *Uromyces fabae*. Fungal Genet. Biol. 1998; 24:77–85. [PubMed: 9742194]

Howard RJ, Valent B. Breaking and entering: host penetration by the fungal rice blast pathogen *Magnaporthe grisea*. Annu. Rev. Microbiol. 1996; 50:491–512. [PubMed: 8905089]

Idrissi FZ, Grotsch H, Fernandez-Golbano IM, Presciatto-Baschong C, Riezman H, Geli MI. Distinct acto/myosin-I structures associate with endocytic profiles at the plasma membrane. J. Cell Biol. 2008; 180:1219–1232. [PubMed: 18347067]

Jeon J, Goh J, Yoo S, Chi MH, Choi J, Rho HS, et al. A putative MAP kinase kinase kinase, MCK1, is required for cell wall integrity and pathogenicity of the rice blast fungus, *Magnaporthe oryzae*. Mol. Plant Microbe Interact. 2008; 21:525–534. [PubMed: 18393612]

Kaksonen M, Sun Y, Drubin DG. A pathway for association of receptors, adaptors, and actin during endocytic internalization. Cell. 2003; 115:475–487. [PubMed: 14622601]

Kaksonen M, Toret CP, Drubin DG. Harnessing actin dynamics for clathrin-mediated endocytosis. Nat. Rev. Mol. Cell Bio. 2006; 7:404–414. [PubMed: 16723976]

Kim JH, Kim HW, Heo DH, Chang M, Baek IJ, Yun CW. FgEnd1 is a putative component of the endocytic machinery and mediates ferrichrome uptake in *Fusarium graminearum*. Curr. Genet. 2009; 55:593–600. [PubMed: 19756628]

Lee K, Singh P, Chung WC, Ash J, Kim TS, Hang L, Park S. Light regulation of asexual development in the rice blast fungus, *Magnaporthe oryzae*. Fungal Genet. Biol. 2006; 43:694–706. [PubMed: 16765070]

Lee SC, Schmidtke SN, Dangott LJ, Shaw BD. *Aspergillus nidulans* ArfB plays a role in endocytosis and polarized growth. Eukaryot. Cell. 2008; 7:1278–1288. [PubMed: 18539885]

Li SJ, Myung K, Guse D, Donkin B, Proctor RH, Grayburn WS, Calvo AM. FvVE1 regulates filamentous growth, the ratio of microconidia to macroconidia and cell wall formation in *Fusarium verticillioides*. Mol. Microbiol. 2006; 62:1418–1432. [PubMed: 17054442]

Pelham HR. SNAREs and the secretory pathway-lessons from yeast. Exp. Cell Res. 1999; 247:1–8. [PubMed: 10047442]

Penalva MA. Endocytosis in filamentous fungi: Cinderella gets her reward. Curr. Opin. Microbiol. 2010; 13:684–692. [PubMed: 20920884]

Raths S, Rohrer J, Crausaz F, Riezman H. end3 and end4: two mutants defective in receptor-mediated and fluid-phase endocytosis in *Saccharomyces cerevisiae*. J. Cell Biol. 1993; 120:55–65. [PubMed: 8380177]

Read ND, Kalkman ER. Does endocytosis occur in fungal hyphae? Fungal Genet. Biol. 2003; 39:199–203. [PubMed: 12892632]

Shaw BD, Chung DW, Wang CL, Quintanilla LA, Upadhyay S. A role for endocytic recycling in hyphal growth. Fungal. Biol. 2011; 115:541–546. [PubMed: 21640317]

Skamnioti P, Henderson C, Zhang Z, Robinson Z, Gurr SJ. A novel role for catalase B in the maintenance of fungal cell-wall integrity during host invasion in the rice blast fungus *Magnaporthe grisea*. Mol. Plant Microbe Interact. 2007; 20:568–580. [PubMed: 17506334]

Smythe, E.; Ayscough, KR. EMBO Rep. 2003. The Ark1/Prk1 family of protein kinases. Regulators of endocytosis and the actin skeleton; p. 246-251.

Song WW, Dou XY, Qi ZQ, Wang Q, Zhang X, Zhang HF, Guo M, Dong SM, Zhang ZG, Wang P, Zheng XB. R-SNARE homolog MoSec22 is required for conidiogenesis, cell wall integrity, and pathogenesis of *Magnaporthe oryzae*. PLoS One. 2010; 5:e13193. [PubMed: 20949084]

Steinberg G. On the move: endosomes in fungal growth and pathogenicity. Nat. Rev. Microbiol. 2007; 5:309–316. [PubMed: 17325725]

Talbot NJ, Foster AJ. Genetics and genomics of the rice blast fungus *Magnaporthe grisea*: Developing an experimental model for understanding fungal diseases of cereals. Adv. Bot. Res. 2001; 34:263–287.

Thines E, Weber RW, Talbot NJ. MAP kinase and protein kinase A-dependent mobilization of triacylglycerol and glycogen during appressorium turgor generation by *Magnaporthe grisea*. Plant Cell. 2000; 12:1703–1718. [PubMed: 11006342]

Toret CP, Drubin DG. The budding yeast endocytic pathway. J. Cell Sci. 2006; 119:4585–4587. [PubMed: 17093262]

Upadhyay S, Shaw BD. The role of actin, fimbrin and endocytosis in growth of hyphae in *Aspergillus nidulans*. Mol. Microbiol. 2008; 68:690–705. [PubMed: 18331474]

Valent B, Farrall L, Chumley FG. *Magnaporthe grisea* genes for pathogenicity and virulence identified through a series of backcrosses. Genetics. 1991; 127:87–101. [PubMed: 2016048]

Verdin J, Bartnicki-Garcia S, Riquelme M. Functional stratification of the Spitzenkörper of *Neurospora crassa*. Mol. Microbiol. 2009; 74:1044–1053. [PubMed: 19843220]

Virag A, Harris SD. The Spitzenkörper: a molecular perspective. Mycol. Res. 2006; 110:4–13. [PubMed: 16378719]

Wang P, Shen G. The endocytic adaptor proteins of pathogenic fungi: charting new and familiar pathways. Medical Mycol. 2011; 49:449–457.

Zhang HF, Liu KY, Zhang X, Song WW, Zhao Q, Dong YH, Guo M, Zheng XB, Zhang ZG. A two-component histidine kinase, MoSLN1, is required for cell wall integrity and pathogenicity of the rice blast fungus, *Magnaporthe oryzae*. Curr. Genet. 2010; 56:517–528. [PubMed: 20848286]

Zhang HF, Liu KY, Zhang X, Tang W, Wang JS, Guo M, Zhao Q, Zheng XB, Wang P, Zhang ZG. Two phosphodiesterase genes, PDEL and PDEH, regulate development and pathogenicity by modulating intracellular cyclic AMP levels in *Magnaporthe oryzae*. PLoS One. 2011a; 6:e17241. [PubMed: 21386978]

Zhang HF, Tang W, Liu KY, Huang Q, Zhang X, Yan X, Chen Y, Wang JS, Qi ZQ, Wang ZY, Zheng XB, Wang P, Zhang ZG. Eight RGS and RGS-like proteins orchestrate growth, differentiation, and pathogenicity of *Magnaporthe oryzae*. PLoS Pathog. 2011b; 7:e1002450. [PubMed: 22241981]

Zhang LS, Lv RL, Dou XY, Qi ZQ, Hua CL, Zhang HF, Wang ZY, Zheng XB, Zhang ZG. The function of MoGlk1 in integration of glucose and ammonium utilization in *Magnaporthe oryzae*. PLoS One. 2011c; 6:e22809. [PubMed: 21818394]

Zhu YY, Chen HR, Fan JH, Wang YY, Li Y, Chen JB, Fan JX, Yang SS, Hu LP, Leung H, Mew TW, Teng PS, Wang ZH, Mundt CC. Genetic diversity and disease control in rice. Nature. 2000; 406:718–722. [PubMed: 10963595]

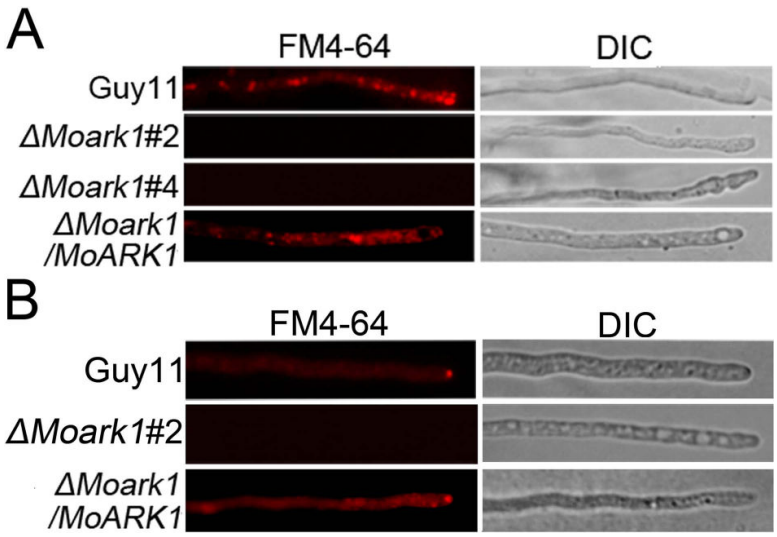

Figure 1.

MoArk1 has a role in formation of the Spitzenkörper and endocytosis.

(A) FM4-64 staining revealed that the Δ*Moark1* mutant was defective in endocytosis. Strains were grown for 2 days on the CM-overlaid microscope slides before adding FM4-64 and photographs were taken after 15 min exposure to FM4-64. Camera exposure is indicated in seconds. (B) The wild type and the complemented strains showed the presence of an intact Spitzenkörper at the tips of the hyphae, which was missing in the Δ*Moark1* mutants after exposure to FM4-64 staining for 15 min. Strains were grown for 2 days on CM-overlaid microscope slides before staining.

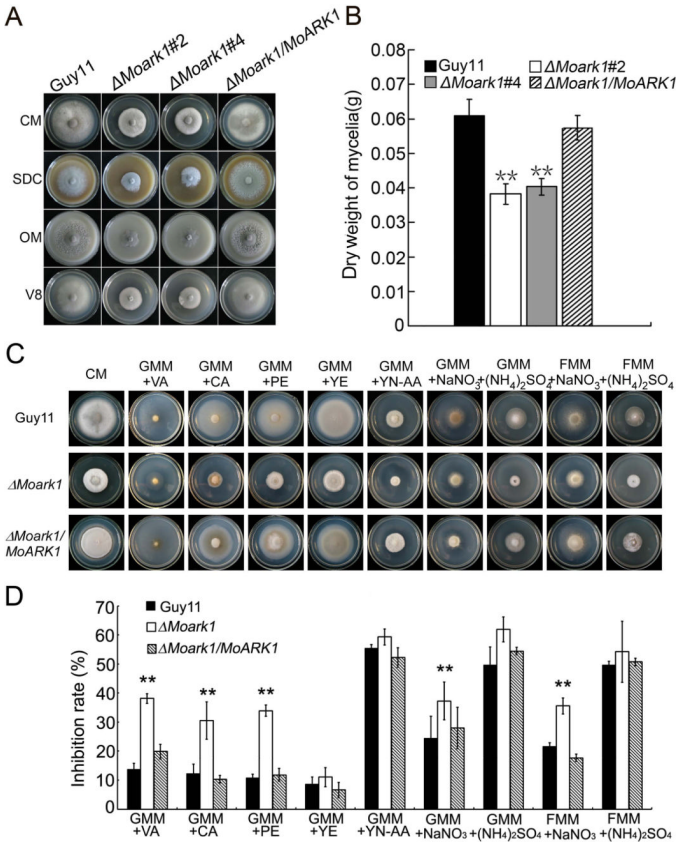

Figure 2.

MoArk1 is required for normal mycelial growth on various media.

(A) The Δ*Moark1* mutants displayed reduced mycelial growth on CM (complete medium), SDC (straw decoction and corn agar), OM (oatmeal agar) and V8 medium following incubation of plates at 28°C for 7 days in the dark. (B) Mycelium dry weight assessment of Δ*Moark1* mutants, wild type and complemented strains (Δ*Moark1/MoARK1*) cultures. (C) Supplements, such as vitamins, casamino acids (CA), peptone (PE), yeast extract (YE) and yeast nitrogen base without amino acids (YN-AA), were added in the same amounts to GMM (containing 10 mM NH_4^+) to determine what component(s) of CM remediated Δ*Moark1* growth. Besides, 100 mM $NaNO_3$ or 50 mM $(NH_4)_2SO_4$ was added to 1% glucose or 1% fructose to compare the different monosaccharide absorption differences. (D) Statistical analyses of the inhibition rate of wild type Guy11, Δ*Moark1* mutant and the complemented strains on different sole nitrogen and carbon sources. Error bars represent the standard deviations and asterisks denote statistical significances (p<0.01).

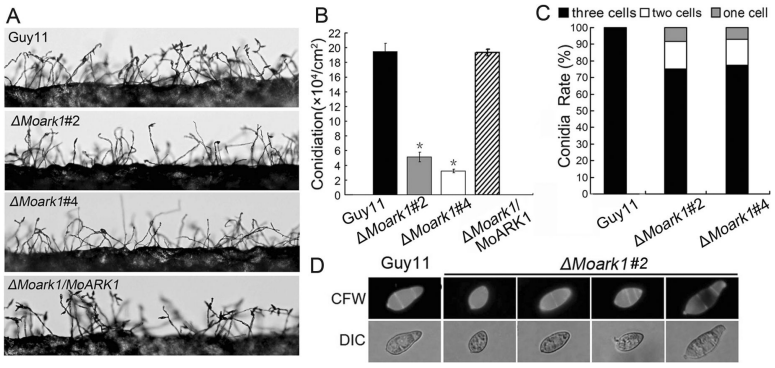

Figure 3.

The Δ*Moark1* deletion mutants show abnormal conidial morphology and reduced conidiation.

(A) Development of conidia on conidiophores is affected by *MoARK1* disruption. Strains grown on SDC medium for 7 days were examined by light microscopy. (B) Statistical analysis of conidia production. The conidia produced by the wild type strain (Guy11), the mutants and complemented strains grown on SDC medium for 10 days were collected, counted, and analyzed by Duncan analysis ($p<0.01$). Asterisks indicate significant differences among Guy11, the Δ*Moark1* mutant and complemented strains. Error bars represent standard deviation (n=3). Three independent experiments yield similar results. Error bars represent standard deviation (n=3). (C) The percentage of each type of abnormal conidia (n=100). Three independent experiments were performed and similar results were obtained. (D) Conidia shape comparison. The conidia were stained with calcofluor white and photographed.

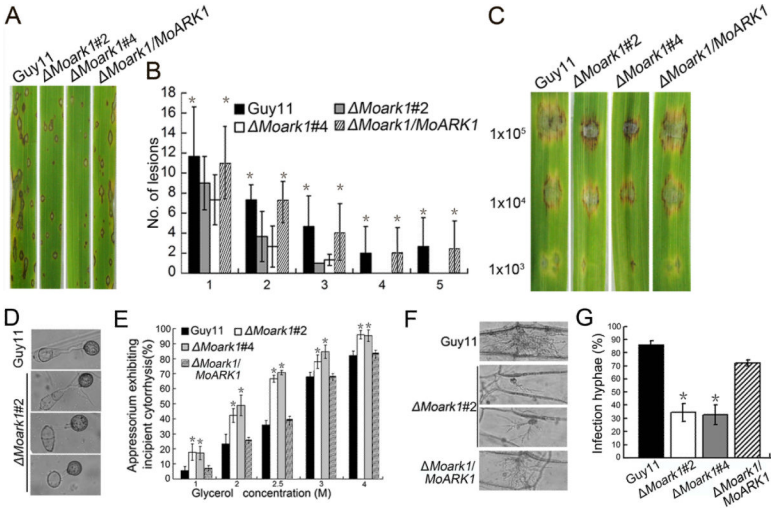

Figure 4.

MoARK1 deletion attenuated pathogenicity.

(A) The *MoARK1* deletion attenuated pathogenicity on rice leaves. (B) Quantification of lesion type (0 = no lesion; 1 = pinhead-sized brown specks; 2 = 1.5 mm brown spots; 3 = 2–3 mm gray spots with brown margins; 4 = many elliptical gray spots longer than 3 mm; 5 = coalesced lesions infecting 50% or more of the leaf area), reveals no difference in lesion types 1–3, however, the Δ*Moark1* mutants do not make any lesion types 4 and 5. Lesions were photographed and measured or scored 7 dpi and experiments were repeated twice with similar results. n=35 for each mutant. (C) Conidia containing different concentration of Δ*Moark1* mutants, were drop-inoculated onto barley and show a virulence defect compared to wild type strain (Guy11) and complemented strains, as manifested by smaller lesions at 5 dpi. (D) Appressoria formation is altered in the Δ*Moark1* mutant. (E) Collapsed appressoria were observed in the wild type Guy11, Δ*Moark1* mutant, and complemented strains. For each glycerol concentration, at least 100 appressoria were observed and numbers of collapsed appressoria were counted. (F) The Δ*Moark1* mutants exhibited reduced host penetration on onion epidermis after 48 h in contrast with control strains. (G) Quantification of hyphae infection on onion epidermis after 48 h. Three independent biological experiments yielded similar results. Error bars represent standard deviation, and asterisks represent significant difference between Guy11 and mutants ($p<0.01$).

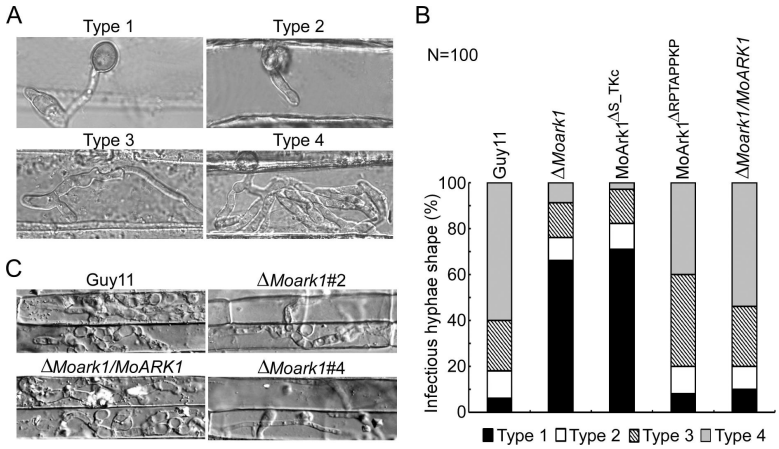

Figure 5.

Conolization of Δ*Moark1* mutant on plants

(A) Close observation of infectious growth on barley. Excised barley leaves from 7-day-old barley seedlings were inoculated with conidial suspension (1×10^4 spores/ml of each strain). Infectious growth was observed at 24 hpi. (B) Statistics analysis for each type of infectious hypha shape, for each tested strain, 100 infecting hypha (n=100) were counted per replicate, and the experiment repeated three times. (C) Excised rice sheath from 4-week-old rice seedlings was inoculated with conidial suspension (1×10^4 spores/ml of each strain). Infectious growth was observed at 48 hpi.

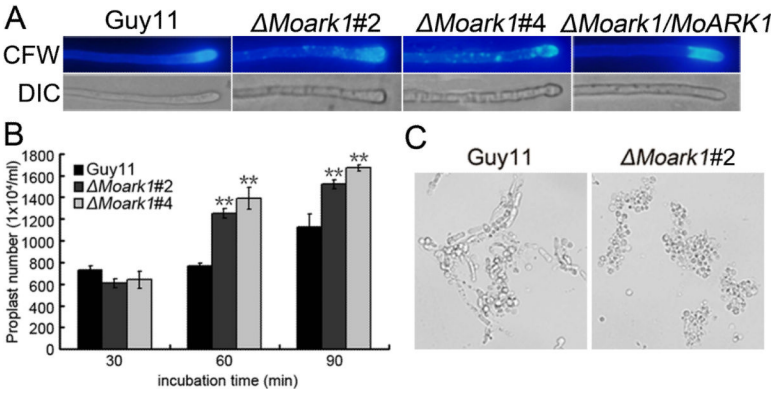

Figure 6.

Mycelial CFW staining and protoplast release assay.

(A) Disruption of *MoARK1* altered the distribution of chitin on the cell wall. Wild-type and mutant hyphae were stained with 10 μg/ml CFW for 5 min without light before being photographed. The experiment was repeated three times with triplicate and displayed the same results. (B) Protoplast release assay of Guy11 and Δ*Moark1* mutants. Asterisks indicate a significant different between the mutants and wild type strain at $p<0.01$, according to the Duncan's range test. (C) Light microscopic examination of protoplast release after 40 minutes.

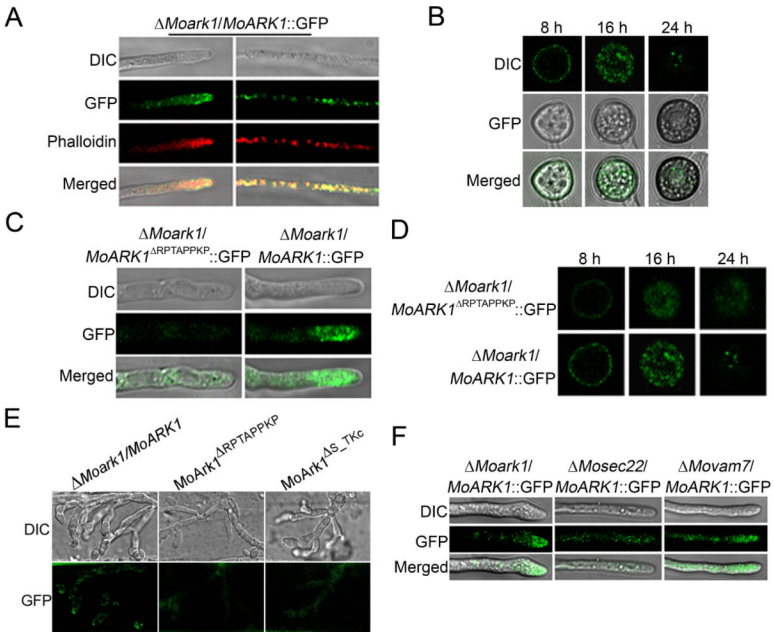

Figure 7.

Cellular localization of MoArk1-GFP and MoArk1$^{\Delta RPTAPPKP}$-GFP.

(A) Vegetative hyphae tips were observed under laser scanning confocal microscopy. The hyphae were stained with the actin dye rhodamine-phalloidin after 48 h static culture. DIC, differential interference contrast image. (B) Δ*Moark1*/MoArk1-GFP fluorescence observation in appressoria formation process after 8, 16, and 24 h under Laser scanning confocal microscopy. (C) Vegetative hyphae tips of Δ*Moark1*/MoArk1$^{\Delta RPTAPPKP}$-GFP were observed under laser scanning confocal microscopy. (D) Δ*Moark1*/ MoArk1$^{\Delta RPTAPPKP}$-GFP fluorescence observation in appressoria formation process after 8, 16, and 24 h under laser scanning confocal microscopy.

(E) Invasive hyphae produced by the *MoARK1*-GFP, *MoARK1*$^{\Delta RPTAPPKP}$-GFP and *MoARK1*$^{\Delta S\_TKc}$-GFP transformants in onion epidermal cells were examined 24 hpi.

(F) Vegetative hyphae tips of Δ*Moark1*/*MoARK1*, Δ*Mosec22*/*MoARK1* and Δ*Movam7*/*MoARK1* were observed under Laser scanning confocal microscopy.

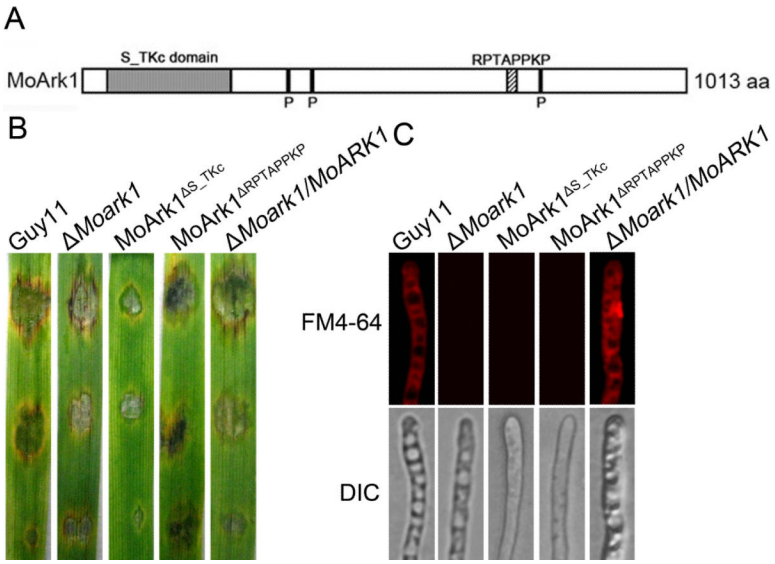

Figure 8.

Function of S/TKc domain and RPTAPPKP motif.

(A) Prediction domains of MoArk1. (B) Pathogenicity of mutant MoArk1$^{\Delta S/TKc}$ and MoArk1$^{\Delta RPTAPPKP}$. (C) FM4-64 staining of mutant MoArk1$^{\Delta S/TKc}$ and MoArk1$^{\Delta RPTAPPKP}$ revealed that they were defective in endocytosis.